Manipulation of the overall polarization orientation in the focal volume of high numerical objectives

Jiannong Chen (陈建农)*, **Linwei Zhu** (朱林伟), **and Zhigang Li** (李志刚)

School of Physics and Opto-electronics Engineering, Ludong University, Yantai 264025, China
*Corresponding author: 13220935107@163.com

We propose an approach for tuning the three-dimensional polarization of a focusing subwavelength spot by a high numerical aperture objective. The incident beams are composed of a radially polarized beam, an azimuthally polarized beam, and a linearly polarized beam with three different weighting factors, respectively. A specially designed adjustable amplitude angular selector is also inserted at the back aperture of the objective for tuning the polarization azimuthally. It is shown that any desired overall polarization orientation can be obtained. We calculated the overall polarization orientation in the focal volume. It is found that the polar angle of the overall polarization orientation can be arbitrarily tuned by the combination of a radially polarized beam and a linearly polarized beam with different weighting factors, and the azimuthal angle can be tuned by rotating the orientation of the linearly polarized beam azimuthally.

OCIS codes: 050.1940, 130.5440, 260.0260.
doi: 10.3788/COL201816.010501.

The far-field focusing investigation by a high numerical objective (OB) has long been an attractive topic[1–10]. The tightly focused subwavelength spot, an either transversely[1] or axially super resolved spot[7], or a specially shaped focal spot, such as a doughnut-like spot[4,11], a long-needle-like spot[9,12], or a complete spiral spot[10], can always find potential applications in various fields, such as high-resolution optical microscopic fluorescence imaging[12,13], optical trapping and manipulation[14–16], optical data storage[17], optical lithography[18], plasmonic wave excitation[19], and metamaterial fabrication[20]. Most of the applications are polarization-sensitive. For example, the probes of near-field scanning optical microscopy (NSOM) are illuminated with the focusing spot of the OB[21]. The electric-field enhancement at the tip of the probe is highly sensitive to the polarization of the illuminating focusing spot. Another polarization-sensitive application is the single dipolar molecule detection or nanorod orientation detection. The fluorescent emission efficiency of dipolar molecules or nanorods strongly depends on the polarization direction of the external excitation field[22]. In recent years, many investigations about the polarization structuring, polarization controlling, and polarization characterization are reported. Abouraddy and Toussaint proposed a theory and the implementation approach for creating the elliptical polarization at some planes of the focal volume in microscopy[23]. In 2006, Bomzon's research shows that, when a circularly polarized plane wave is focused by a high NA OB, a geometrical phase is added to the wave front, and the polarization of the wave front in the focal plane is space-varying[24]. In the next year, Bomzon and Gu also reported that the depolarization occurred in focusing cylindrical light beams accompanied by a space-varying geometrical phase. This phase results in the formation of modes with helicities and phase singularities that differ from those of the original beam[25]. In 2007, Iglesias and Vohnsen show that the polarization structuring can shape the focal intensity in high-resolution microscopy[26]. In 2010, the polarization characterizations of the focal volume of the high NA OB are presented[27]. It is found that, by adjusting the incident polarizations of laser beams, the apodization of an OB, and the NA of an OB, the focal fields with either a dominant transverse component or a longitudinal component can be generated, providing a means of light–matter interaction with one particular polarization component in the focal volume. In addition, it is discovered that polarization distributions with three polarization components of the same strength are possible.

In 2012, Gu and his group reported that, by configuring the weighted radially polarized beam and azimuthally polarized beam along with a mainly azimuthal controllable apodizer, they realized the three-dimensionally adjustable overall polarization orientation at the focal plane[28]. Using the sparsely distributed nanorod solution on the substrate, they further detected the orientation of a single nanorod through imaging and melted the nanorod when the nanorod orientation is parallel to the overall polarization direction by applying a strong femtosecond pulse laser. In this reference, the overall polarization is defined by calculating the comprehensive effect contributed by all local polarization in the focal plane. The other local polarization influence out of the focal plane in the focal volume is not taken into account. However, the electric field presents at any points in the focal volume the size of which usually ranges from several hundreds of nanometers to several micrometers. Furthermore, the surface of the half-value of the maximum intensity in the focal volume could take on various shapes. When considering the interaction with the

nanorods or single molecule, the nanorods or single molecule may be larger or smaller than the size of the focal volume enclosed by the surface of the half-value of the maximum intensity. The interaction with the nanorods or relatively a large molecule should be the collective role of electrical fields at all points in the focal volume. The precise knowledge or control of interaction between the electric field with specific overall polarization in the focal volume and nanorod or single molecule orientation requires further detailed investigation.

In this study, we direct the radially polarized beam, azimuthally polarized beam, and linearly polarized beam with an adjustable respective weighting factor into the high NA OB along with an azimuthally oriented angular selector. We simulated the polarization vector and intensity distribution in three-dimensional space in different combinations of three weighting factors and an azimuthally different oriented angular selector. The overall polarization orientation parameters of the focal volume are defined and calculated. We show how the azimuthal angle and the polar angle of the overall polarization orientation of the focal volume can be expectedly manipulated.

When the radially polarized beam, azimuthally polarized beam, and x-axis polarized beam are focused with the same OB, three components in the focal volume can be expressed as

$$\vec{E}_x = (\gamma E_{xr} + \delta E_{xa} + \beta E_{xl})\vec{e}_x, \tag{1}$$

$$\vec{E}_y = (\gamma E_{yr} + \delta E_{ya} + \beta E_{yl})\vec{e}_y, \tag{2}$$

$$\vec{E}_z = (\gamma E_{zr} + \delta E_{za} + \beta E_{zl})\vec{e}_z, \tag{3}$$

where γ, δ, and β are the weighting factors. Before being directed into the OB, the laser beam is collimated and split into three beams with a continuously tunable intensity weighting factor. They are converted into a radially polarized beam, an azimuthally polarized beam, and a linearly polarized beam, respectively. After polarization conversion, the three beams are combined, aligned, and then directed into the OB. Figure 1 shows the schematic diagram for the overall polarization manipulation. An azimuthally controllable angular selector, as shown in the inset, is inserted into the back aperture of the OB. $0 \leq \varepsilon \leq 2\pi$, and $0 \leq \zeta \leq 2\pi$. The angular selector serves as an amplitude filter, which could determine the azimuthal angle of the overall polarization orientation in the focal volume.

In our investigation, we consider characterization and manipulation of the overall polarization orientation in a focal volume of the high numerical OB. We propose the following definition for calculating and characterizing the three electric-field components. The intensity in any points indexed by (i, j, l) can be expressed as

$$I(i,j,l) = \{\text{abs}[E_x(i,j,l)]\}^2 + \{\text{abs}[E_y(i,j,l)]\}^2$$
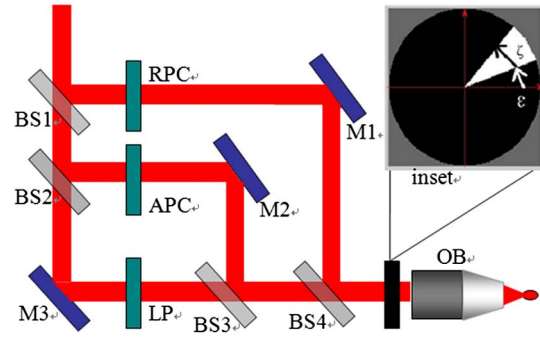$$+ \{\text{abs}[E_z(i,j,l)]\}^2. \tag{4}$$

Fig. 1. Schematic diagram for overall polarization manipulation. The inset is an azimuthally adjustable angular selector as the amplitude filter inserted at the back aperture of the OB. ε and ζ are changeable. The BS1, BS2, BS3, and BS4 are the beam splitters, and M1, M2, and M3 are the mirrors. RPC, APC, and LP are radial polarization converter, azimuthal polarization converter, and linear polarizer, respectively.

When $I(i,j,l) < 0.5I_{\max}$, we let $E_x(i,j,l) = 0$, $E_y(i,j,l) = 0$. and $E_z(i,j,l) = 0$. Then, we define E_{x_total}, E_{y_total}, and E_{z_total} as follows:

$$E_{x\_\text{total}} = \sum_{i=1}^{M}\sum_{j=1}^{M}\sum_{l=1}^{N} |E_x(i,j,l)| \frac{\text{Re}[E_x(i,j,l)]}{|\text{Re}[E_x(i,j,l)]|}, \tag{5}$$

$$E_{y\_\text{total}} = \sum_{i=1}^{M}\sum_{j=1}^{M}\sum_{l=1}^{N} |E_y(i,j,l)| \frac{\text{Re}[E_y(i,j,l)]}{|\text{Re}[E_y(i,j,l)]|}, \tag{6}$$

$$E_{z\_\text{total}} = \sum_{i=1}^{M}\sum_{j=1}^{M}\sum_{l=1}^{N} |E_z(i,j,l)| \frac{\text{Re}[E_z(i,j,l)]}{|\text{Re}[E_z(i,j,l)]|}. \tag{7}$$

The overall transverse component can be calculated as

$$E_{r\_\text{total}} = \sqrt{E_{x\_\text{total}}^2 + E_{y\_\text{total}}^2}. \tag{8}$$

The azimuthal angle of the overall polarization is defined as

$$\varphi_{\text{total}} = \arctan\left(\frac{E_{y\_\text{total}}}{E_{x\_\text{total}}}\right). \tag{9}$$

The orientation polar angle with respect to the z axis can be defined as

$$\theta_{\text{total}} = \frac{\pi}{2} - \arctan\left(\frac{E_{z\_\text{total}}}{E_{r\_\text{total}}}\right). \tag{10}$$

To verify the effectiveness of the calculation methods described above, we first calculated three cases of the polarization orientation of the focal spot when each of a pure radially polarized beam, a pure azimuthally polarized beam, and a pure x-axis linearly polarized beam is focused without an amplitude angular selector at the back aperture of a high NA OB using the vector diffraction
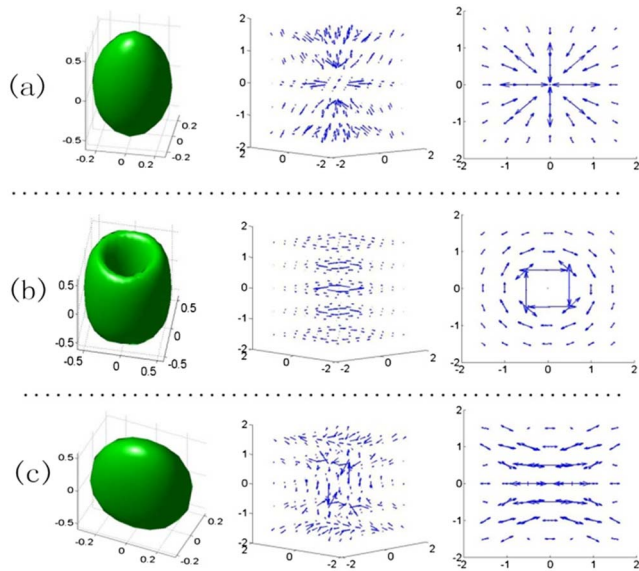
Fig. 2. Three-dimensional intensity and polarization distribution in the focal volume and two-dimensional polarization distribution in the focal plane. (a) Pure radially polarized beam; (b) pure azimuthally polarized beam; (c) pure x-axis polarized beam. First column is the intensity distributions; second column is the perspective views of polarization distribution; third column is the top view of polarization distribution in the focal plane.

theory[5,28] and the equations described above. Figure 2 shows the three-dimensional intensity and polarization distribution of each individual beam in the focal volume and two-dimensional polarization in the focal plane. It can be seen that, in each of three situations, the overall polarization orientation is easily predictable. It should be denoted here that the NA of the OB is 0.95 in the simulation, and the length scale unit is wavelength in all figures throughout this Letter. Figure 3 shows the simulation results of three cases. In Fig. 3(a), we see that the overall polarization orientation is pointing along the z axis with the transverse component being zero as expected when a pure radially polarized beam is focused. In Fig. 3(b), both the azimuthal angle and polar angle of the overall polarization are zero with the negligible magnitude when a pure azimuthally polarized beam is focused. There is no longitudinally polarized component as anticipated. The transversely polarized component can be canceled because of the circular symmetry as illustrated in Fig. 3(b). In Fig. 3(c), when a pure x-axis linearly polarized beam is focused, the overall polarization orientation is along the x axis as expected. It is demonstrated that our definition and calculation method of the overall polarization orientation is effective for describing the property of electric fields in a three-dimensional focal volume within the equal-intensity surface of half-maximum intensity.

To manipulate the overall polarization orientation azimuthally, we use the combination of a pure uniform azimuthally polarized beam with a weighting factor of 0.9, a pure uniform radially polarized beam with a weighting factor of 0.1, and an azimuthally adjustable angular selector. The parameters of the angular selector illustrated in Fig. 1 are as follows: $\zeta = \pi/6$, $\varepsilon = -\pi/12$, $5\pi/12$, $11\pi/12$, and $17\pi/12$. The calculation results are shown in Fig. 4. The azimuthal angle and polar angle are $-95°$ and $-4°$, respectively, in Fig. 4(a), $-5°$ and $-4°$, respectively, in Fig. 4(b), 84°, and $-4°$, respectively, in Fig. 4(c), $-174°$ and $-4°$, respectively, in Fig. 4(d). In four situations, the polar angle with respect to the z axis remains the same; however, the azimuthal angle of the overall polarization
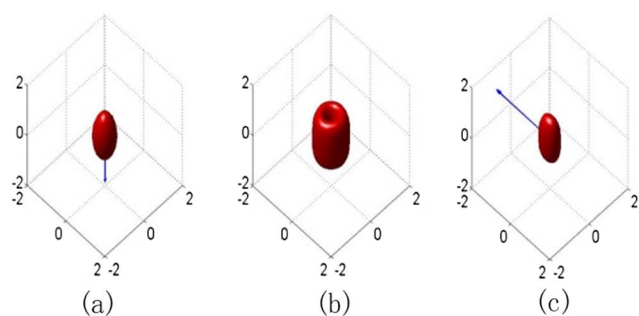

Fig. 3. Overall polarization orientation in the focal volume: (a) the incident beam is a pure radially polarized beam. The blue arrow denoting the polarization direction is oriented with a polar angle of 90°; (b) the incident beam is a pure uniform azimuthally polarized beam. There is no longitudinally polarized component. In the volume enclosed with the surface of equal intensity, which is half of the maximum intensity, the local transverse components canceled each other. There is also no transversely polarized component in the volume; (c) a pure uniform x-axis polarized beam generates an overall x-axis polarized component when it is focused by an OB.
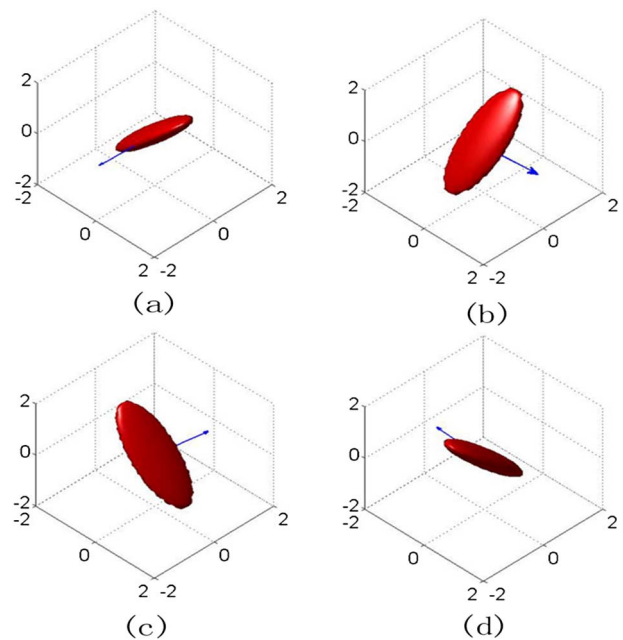

Fig. 4. Manipulation of the azimuthal angle of the overall polarization orientation by the combination of a pure uniform azimuthally polarized beam with a weighting factor of 0.9, a pure uniform radially polarized beam with a weighting factor of 0.1, and an azimuthally adjustable angular selector.

orientation changes with the rotation of the adjustable angular selector. It is found that the intensity distribution is also azimuthally rotated. Here, it is necessary to note that the shape of the focal spot is the same, except that the orientation of intensity distribution is azimuthally rotated. This rotation is caused by the azimuthally adjustable angular selector. The shape of the focal spot is completely determined by the two purely different polarized beams and their respective weighting factors.

To tune the polar angle of the overall polarization orientation, we use the combination of a pure uniform linearly polarized beam and a pure uniform radially polarized beam. With different weighting factors and the angular selector parameters of $\zeta = 2\pi$ and $\varepsilon = 0$, the polar angle with respect to the z axis can be tuned arbitrarily. Figure 5 demonstrates the calculation results. In Fig. 5(a), the weighting factors of the radially polarized beam and the linearly polarized beam are 0.9 and 0.1, respectively, and the corresponding azimuthal angle and polar angle are $-180°$ and $-65°$, respectively. In Fig. 5(b), the weighting factors of the radially polarized beam and the linearly polarized beam are 0.7 and 0.3, respectively, and the corresponding azimuthal angle and polar angle are $-180°$ and $-30°$, respectively. In Fig. 5(c), the weighting factors of the radially polarized beam and the linearly polarized beam are 0.5 and 0.5, respectively, and the corresponding azimuthal angle and polar angle are $-180°$ and $-15°$, respectively. In Fig. 5(d), the weighting factors of the
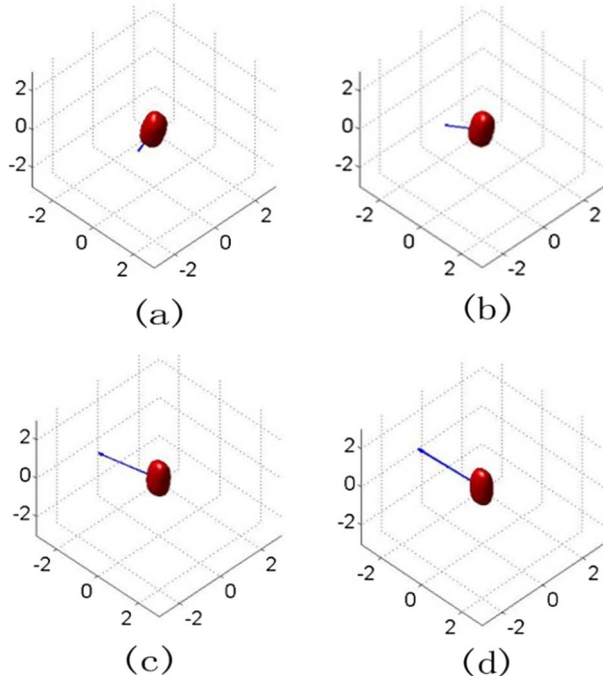

Fig. 5. Manipulation of the polar angle of the overall polarization orientation by the combination of a pure uniform radially polarized beam and a pure uniform linearly polarized beam. With different weighting factors and the angular selector parameters of $\zeta = 2\pi$ and $\varepsilon = 0$, the polar angle can be tuned arbitrarily.

radially polarized beam and the linearly polarized beam are 0.3 and 0.7, respectively, and the corresponding azimuthal angle and polar angle are $-180°$ and $-7°$, respectively.

To tune both the polar angle and azimuthal angle of the overall polarization orientation simultaneously, we propose two approaches: the first approach is to adjust both of the ratios of the azimuthally polarized beam to the radially polarized beam and the azimuthal angle of the angular selector orientation. For example, if we choose $\zeta = \pi/6$, $\varepsilon = -\pi/12$, and set different ratios of azimuthally polarized beams to radially polarized beams, we will obtain different azimuthal angle and polar angle values. If we choose $\zeta = \pi/6$, $\varepsilon = -5\pi/12$, and set different ratios of azimuthally polarized beams to radially polarized beams, we will certainly get another set of azimuthal angle and polar angle values; the second approach is to use the combination of a pure uniform linearly polarized beam and a pure uniform radially polarized beam. As illustrated in Fig. 5, the polar angle can be tuned by changing the ratios of a pure uniform radially polarized beam to a pure uniform linearly polarized beam. If, at the same time, we rotate the orientation of the linearly polarized beam azimuthally, then it is certain that both the polar angle and the azimuthal angle of the overall orientation can be expectedly and arbitrarily manipulated. Compared to the first approach, the second approach is much easier to implement in practice.

However, the discussion and calculation above is mainly about that; when we give the types of two or more differently polarized beams and their respective weighting factors along with the parameters of the angular selector, we calculate the azimuthal angle and polar angle of the overall polarization orientation in the defined focal volume. Conversely, we may naturally ask what kinds of polarized beams and weighting factors there should be if a given azimuthal angle and polar angle of the overall polarization orientation need to be obtained. To resolve this issue, we choose the combination of the radially polarized beam and linearly polarized beam as the input beam. As the radially polarized beam is circularly symmetrical beam, it is obvious that the azimuthal angle of the overall polarization orientation depends completely on the azimuthal orientation of the linearly polarized beam. It can be easily realized by rotating the linear polarizer. As for the polar angle of the overall polarization orientation, we calculated many results when a series of combinations of two different weighting factors are used. The results are plotted in the Fig. 6. On the basis of this red line obtained by numerical calculation, an arbitrary point on the line corresponds to the approximate polar angle desired and its respective weighting factor of a radially polarized beam. For example, the point M denoted with a blue box on the line corresponds to the weighting factor $\eta = 0.55$ (radially polarized beam), $\xi = 1 - \eta = 0.45$ (linearly polarized beam), and, accordingly, the polar angle is around 27°. If we want to obtain the polar angle ranging from 0° to $-90°$, the phase of the radially polarized beam should be retarded a value of π.
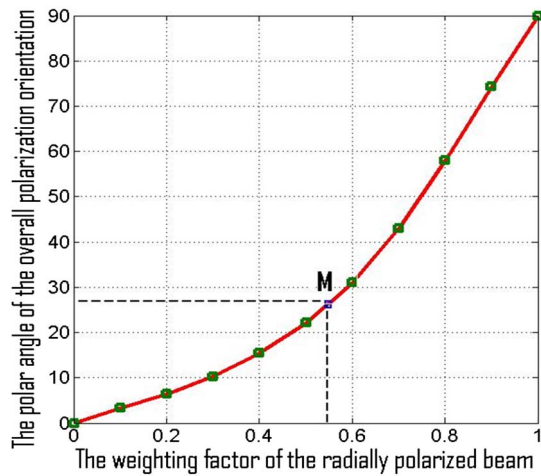
Fig. 6. Curve between the polar angle of the overall polarization orientation and the weighting factor of the radially polarized beam.

In conclusion, we schematically demonstrate a very flexible method for manipulating the overall polarization orientation arbitrarily in the three-dimensional focal volume. By directing three different polarized beams with different weighting factors into the high NA OB, we can arbitrarily control the azimuthal angle and polar angle of the overall polarization orientation in a volume enclosed by a surface on which the intensity is half of the maximum intensity in the focal volume. The definition and the calculation formulas of the overall polarization orientation are given and verified. It is found that the combination of a radially polarized beam and a linearly polarized beam with different weighting factors could result in the tuning of the polar angle. The rotation of the orientation of the linearly polarized beam accordingly can result in the tuning of the azimuthal angle. It is an easy method in implementing the manipulation of the overall polarization orientation.

References

1. R. Dorn, S. Quabis, and G. Leuchs, Phys. Rev. Lett. **91**, 233901 (2003).
2. J. W. M. Chon, X. Gan, and M. Gu, Appl. Phys. Lett. **81**, 1576 (2002).
3. I. J. Cooper, M. Roy, and C. J. R. Sheppard, Opt. Express **13**, 1066 (2005).
4. D. Ganic, X. Gan, and M. Gu, Opt. Express **11**, 2747 (2003).
5. K. S. Youngworth and T. G. Brown, Opt. Express **7**, 77 (2000).
6. G. M. Lerman and U. Levy, Opt. Express **16**, 4567 (2008).
7. H. Lin and M. Gu, Opt. Lett. **36**, 2471 (2011).
8. Q. Zhan and J. R. Leger, Opt. Express **10**, 324 (2002).
9. H. Wang, L. Shi, B. Lukyanchuk, C. Sheppard, and C. T. Chong, Nat. Photon. **2**, 501 (2008).
10. J. Chen, X. Gao, L. Zhu, Q. Xu, and W. Ma, Opt. Commun. **318**, 100 (2014).
11. F. Wackenhut, B. Zobiak, A. J. Meixner, and A. V. Failla, Chin. Opt. Lett. **15**, 030013 (2017).
12. W. Ma, D. Zhang, L. Zhu, and J. Chen, Chin. Opt. Lett. **13**, 052101 (2015).
13. W. Denk, J. H. Strickler, and W. W. Webb, Science **248**, 73 (1990).
14. L. Paterson, M. P. MacDonald, J. Arlt, W. Sibbett, P. E. Bryant, and K. Dholakia, Science **292**, 912 (2001).
15. X. Zhuang, Science **305**, 188 (2004).
16. J. Lamstein, A. Bezryadina, D. Preece, J. C. Chen, and Z. Chen, Chin. Opt. Lett. **15**, 030010 (2017).
17. P. Zijlstra, J. W. M. Chon, and M. Gu, Nature **459**, 410 (2009).
18. Z. Gan, Y. Cao, R. A. Evans, and M. Gu, Nat. Commun. **4**, 2061 (2013).
19. H. Kano, S. Mizuguchi, and S. Kawata, J. Opt. Soc. Am. B **15**, 1381 (1998).
20. C. M. Soukoulis and M. Wegener, Nat. Photon. **5**, 523 (2011).
21. J. M. Gerton, L. A. Wade, G. A. Lessard, Z. Ma, and S. R. Quake, Phys. Rev. Lett. **93**, 180801 (2004).
22. L. Novotny, M. R. Beversluis, K. S. Youngworth, and T. G. Brown, Phys. Rev. Lett. **86**, 5251 (2001).
23. A. F. Abouraddy and K. C. Toussaint, Jr., Phys. Rev. Lett. **96**, 153901 (2006).
24. Z. Bomzon, M. Gu, and J. Shamir, Appl. Phys. Lett. **89**, 241104 (2006).
25. Z. Bomzon and M. Gu, Opt. Lett. **32**, 3017 (2007).
26. I. Iglesias and B. Vohnsen, Opt. Commun. **271**, 40 (2007).
27. H. Kang, B. Jia, and M. Gu, Opt. Express **18**, 10813 (2010).
28. X. Li, T. Lan, C. Tien, and M. Gu, Nat. Commun. **3**, 998 (2012).